Letter

A Unified Model Explaining Heterogeneous Ziegler-Natta Catalysis

Raffaele Credendino, Dario Liguori, Zhiqiang Fan, Giampiero Morini, and Luigi Cavallo

ACS Catal., **Just Accepted Manuscript** • DOI: 10.1021/acscatal.5b01076 • Publication Date (Web): 12 Aug 2015

A Unified Model Explaining Heterogeneous Ziegler-Natta Catalysis

Raffaele Credendino,[1] Dario Liguori,[2] Zhiqiang Fan,[3] Giampiero Morini,[2] Luigi Cavallo,[1,*]

[1] King Abdullah University of Science and Technology (KAUST), Chemical and Life Sciences and Engineering, Kaust Catalysis Center, Thuwal 23955-6900, Saudi Arabia. [2]LyondellBasell Polyolefins, G. Natta Research Center, Piazzale G. Donegani 12, 44100, Ferrara, Italy. [3] Department of Polymer Science and Engineering, MOE Key Laboratory of Macromolecular Synthesis and Functionalization, Zhejiang University, Hangzhou 310027, China. Email: luigi.cavallo@kaust.edu.sa.

Supporting Information Placeholder

ABSTRACT: We propose a model for $MgCl_2$ supported Ziegler-Natta catalysts capable to reconcile the discrepancies emerged in the last 20 years, when experimental data were tried to be rationalized by molecular models. We show that step defects on the neglected but thermodynamically more stable (104) facet of $MgCl_2$ can lead to sites for strong $TiCl_4$ adsorption. The corresponding Ti-active site is stereoeselective, and its stereoselectivity can be enhanced by coordination of Al-alkyls or Lewis bases in the close proximity. The surface energy of the step defected (104) $MgCl_2$ facet is clearly lower than that of the well accepted (110) facet.

Keywords. Heterogeneous Catalysis; Stereoselective Polymerization; Ziegler-Natta Catalysis; Isotactic Polypropylene; DFT calculations.

Despite of the economic relevance of polyolefin commodities, with a volume in the order of 10^6 tons/year and a billionaire market, the intimate nature of the active site of Ziegler-Natta (ZN) catalysts remains elusive. This limited knowledge is consequence of the complex nature of ZN-catalysts, although four key ingredients only compose industrial catalysts. They are the inert $MgCl_2$ support; the catalytically active $TiCl_4$ adsorbed on the $MgCl_2$ surfaces; an Al-alkyl, typically $AlEt_3$, to activate the adsorbed $TiCl_4$; and a Lewis base, either monodentate as benzoates or bidentate as siloxanes, phthalates, 1,3-diethers and succinates, to tune catalytic behaviour and to increase the amount and stereoregularity of the produced polypropylene.[1-4]

The main difficulty in composing this four pieces puzzle is in the uncertainty about the $MgCl_2$ surface(s) hosting the catalytically active Ti-species. Indeed, solved this issue would allow proposing reasonable models, since we have a reasonable knowledge of the local geometry that should be assumed by the catalytically active Ti-species. In this regard, there is consensus that the dominant surface in $MgCl_2$ crystallites, the basal (001) surface corresponding to a plane of Cl atoms, see Figure 1, cannot adsorb $TiCl_4$. Doubts are on which lateral facet hosts the catalytically active Ti-species. The only convergence is on the nature of the two possible facets: the more stable (104)-facet, presenting penta-coordinated Mg atoms, or the less stable (110)-facet, presenting tetra-coordinated Mg atoms,[5-18] see Figure 1.

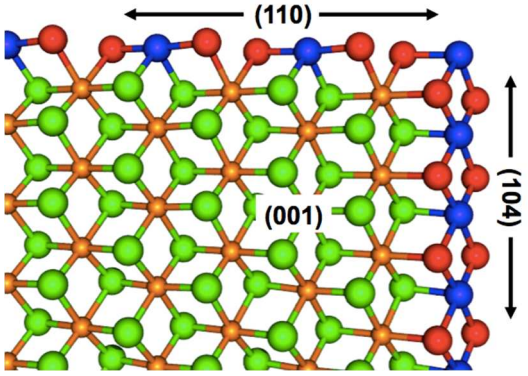

Figure 1. $MgCl_2$ crystallite showing the basal (001) and the lateral (104) and (110)-facets.

Early models, based on the similarity between the (100) and the (110)-facets of $MgCl_2$ and $TiCl_3$ monolayers, suggested that the more stable (104)-facet could host dimeric Ti_2Cl_8 species, with the benefit that the environment around the Ti atoms would mimic the stereoselective sites proposed for $TiCl_3$.[19-23] In this scheme the (110)-facet is not stereoselective, and Lewis bases would posion the (110)-facet preventing $TiCl_4$ adsorption.[24] This scheme dominated the literature for about 20 years since the discovery of supported ZN-catalysts. More recently, severe criticism questioned this scheme. First, a series of static and dynamic DFT calculations indicated that $TiCl_4$ adsorption on the (104)-facet is weak, and formation of dimeric Ti_2Cl_8 is practically impossible.[5,6,8,12,25] Differently, $TiCl_4$ was found to adsorb quite strongly on the (110)-facet. Second, experiments indicated that the Lewis base strongly influences the stereoregularity of the isotactic polypropylene,[26-29] which implies that the Lewis base can coordinate close to the active Ti-species and that it can actively participate in the stereocontrol event. However,

models of the two surfaces indicated that there is no simple way to place a Lewis base in the proximity of the Ti-center on the (104)-facet, while it is simple to imagine a stereoselective role for the Lewis base on the (110)-facet.[10,11,15] Based on these evidences, the (104)-facet was basically abandoned in favour of the (110)-facet, currently considered as the most likely facet active in catalysis.

Unfortunately, even this scenario cannot unify all the experimental knowledge.[18,30-41] The most striking incongruence is the experimental evidence that synthesizing the $MgCl_2$ support in the presence of diisobutyl phthalate or ethyl benzoate leads to the formation of crystallites presenting both 120° and 90° edge angles,[42] the latter indicating the formation of crystallites presenting both the (104) and (110)-facets. Subsequent treatment with $TiCl_4$ generates a catalyst that polymerizes propylene on all the lateral facets of each crystallite.[43] This clearly indicates that polymer can be produced on both the (104) and (110)-facets, at odd with the evidence that $TiCl_4$ cannot adsorb on the (104)-facet, and that there is no model explaining the stereoselective role of the Lewis bases on the (104)-facet.

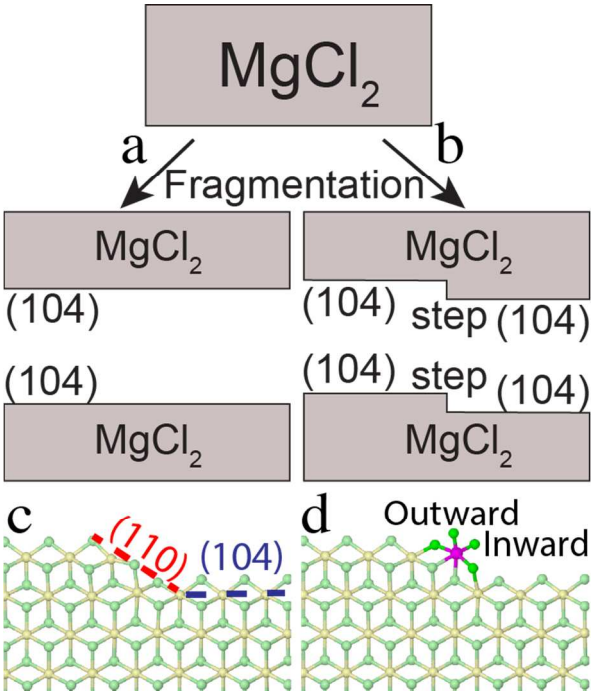

Figure 2. Fragmentation of $MgCl_2$ creating: a) perfect (104)-facets; b) (104)-facets presenting a step-defect; c) geometry of the step-defect on the (104)-facet; d) $TiCl_4$ adsorbed on the (104) step-defect.

Based on DFT calculations[44] we propose a model reconciling all these incongruences. In line with recent efforts focusing on determining low energy defected $MgCl_2$ surfaces,[13,45] we propose a new low energy defect on the (104)-facet that can strongly coordinate $TiCl_4$. The defect we propose allows rationalizing easily the stereoselective role of the Lewis bases also on the (104)-facet. Combined with previous knowledge on the (110)-facet, our results provide a conceptual scheme explaining almost all the knowledge in the field.[46]

Starting from bulk $MgCl_2$ we imagined different fragmentation modes generating perfect or step-defected (104)-facets, see Figure 2. While the perfect (104)-facet corresponds to a perfectly flat surface, the considered defected facet corresponds to have a fragmentation event generating a symmetric step defect on the two surfaces. Comparison between the fragmentation energy of the bulk into the perfect or into step-defected (104)-facets of different size converges in the single step-defect costing only 7.1 kcal/mol, details on the calculation of this value can be found in the Supporting Information. This is value is comparable to the experimental values for the step energy on the Ag(111) or Cu(111)-facets, around 6 kcal/mol per atomic distance.[47,48] Analysis of the step-defected surface shows that the defect corresponds to a junction between the (104) and the (110)-facets, with a local environment capable to host $TiCl_4$ almost epitaxially.

To relate the stability of the step-defected (104)-facet to that of the perfect (104) and (110)-facets, we calculated the surface energy, E_{Surf}, of the perfect (104) and (110)-facets and that of the step-defected (104) facet presenting a variable amount of isolated defects, see the Supporting Information for details. In agreement with previous work,[17] we found that the perfect (104)-facet, with an E_{Surf} of 0.410 J/m^2, is remarkably more stable than the perfect (110)-facet, with an E_{Surf} of 0.722 J/m^2, see Table 1. Interestingly, the E_{Surf} of the (104)-facet presenting 10%, 20% and 30% of isolated step-defects is only 0.429, 0.448 and 0.466 J/m^2, indicating that even a highly defected (104)-facet is clearly more stable than the well accepted (110)-facet. Inclusion of a dispersion term modifies the overall E_{Surf} values, but the trend is the same. Considering that preparation of $MgCl_2$ supports is usually performed under rather drastic conditions, these results indicate that defected surfaces can have a relevant role in Ziegler-Natta catalysis. At this point, we moved to investigate $TiCl_4$ adsorption on the (104) step-defect.

Table 1. Surface energy, E_{Surf} in J/m^2, of perfect (104) and (110)-facets, and of defected (104)-facets presenting a variable amount of step-defects.

	% of defects	E_{Surf}[a]	E_{Surf}[b]
(104)	0	0.410	0.524
(104)	10	0.429	0.539
(104)	20	0.448	0.561
(104)	30	0.466	0.583
(110)	0	0.722	0.912

a) No dispersion term included in the calculations. b) An empirical dispersion term is included in the calculations.

According to calculations, $TiCl_4$ can be accommodated on the (104) step-defect with an overall binding energy of -12.5 kcal/mol, see Figure 2d. This value is much higher than that calculated for $TiCl_4$ adsorption on the perfect (104)-facet, only -2.8 kcal/mol, and it is comparable to that calculated for $TiCl_4$ adsorption on the perfect (110)-facet, -13.9 kcal/mol. Inclusion of dispersion interaction increases these values to -26.8, -12.5 and -25.5 kcal/mol for the (104) step-defect, and for the perfect (104) and (110)-facets, respectively. Consistently with previous work,[5,6,8,12,25] these

numbers indicate that $TiCl_4$ cannot coordinate on the perfect (104)-facet when a disfavorable entropic penalty is considered, while strong coordination on the (104) step-defect or on the (110)-facet is possible also on a free energy level. The good binding of $TiCl_4$ on the (104) step-defect and on the (110)-facet results from having octahedral coordination around the Ti-center, with the slightly stronger coordination of $TiCl_4$ on the (110) surface probably due to a stronger interaction of the coordinated chlorine atoms of $TiCl_4$ with two tetracoordinated Mg atoms, see Figure S1, while $TiCl_4$ coordination on the (104) step-defect involves one tetracoordinated and one pentacoordinated Mg atom, see Figure 2d. Nevertheless, the main conclusion is that a step-defect on the more stable (104) surface is energetically feasible and can adsorb $TiCl_4$ as strong as the (110) facet.

At this point we investigated chain growth, corresponding to propene insertion into the Ti-isobutyl bond (the isobutyl group is used to mimic a polymer chain), at a Ti-center adsorbed on the (104) step-defect. For the sake of simplicity, in all the calculations the configuration of the chiral Ti-center is Λ, and we considered insertion with the chain at both the inward and outward positions, see Figure 2.[46] In both cases we located the transition state for primary and secondary insertion of the *re* and *si* enantiofaces of propene. A cluster model was used to investigate a larger number of cases, while a periodic boundary condition model was used to validate the cluster model and to investigate the impact of an industrially used Lewis base, 9,9-bis(methoxymethyl)-9H-fluorene (BMF).

Table 2. Stereo and regioselectivity of the catalytic sites with nothing, $AlEt_3$ or $AlEt_2Cl$ coordinated next to the Ti-center. $\Delta E^{\ddagger}_{Stereo}$ and $\Delta E^{\ddagger}_{Regio}$ (in kcal/mol) correspond to the energy difference between the transition state for *re* and *si*-propene primary insertion into the Ti-isobutyl bond, $\Delta E^{\ddagger}_{Stereo}$, and for the best secondary versus the best primary transition state for propene insertion into the Ti-isobutyl bond, $\Delta E^{\ddagger}_{Regio}$.

	Nearby species	$\Delta E^{\ddagger}_{Stereo}$	$\Delta E^{\ddagger}_{Regio}$
Cluster model			
Outward	None	0.1	1.2
Inward	None	1.2	1.1
Outward	$AlEt_3$	0.9	1.4
Inward	$AlEt_3$	1.2	1.1
Outward	$AlEt_2Cl$	0.9	1.2
Inward	$AlEt_2Cl$	1.4	1.3
	Nearby species	$\Delta E^{\ddagger}_{Stereo}$	$\Delta E^{\ddagger}_{Regio}$
Periodic model			
Outward	None	0.4	5.3
Inward	None	3.9	5.9
Outward	$AlEt_3$	2.2	6.0
Outward	BMF	5.8	6.1

According to calculations using the cluster model, primary insertion on the resulting catalytic site is not stereoselective if the growing chain is in the outward coordination position, with a $\Delta E^{\ddagger}_{Stereo}$ of only +0.1 kcal/mol, see Table 2, while it is slightly stereoselective if the growing chain is in the inward coordination position, with a $\Delta E^{\ddagger}_{Stereo}$ of +1.2 kcal/mol. Both catalytic sites are scarcely regioselective, with a $\Delta E^{\ddagger}_{Regio}$ around 1 kcal/mol. This result is expected, since no steric hindrance is restricting the conformational space available to the outward growing chain, while only the chlorine atom indicated by a star in Figure 3, is somewhat restricting the conformational space available to the inward growing chain.

Next we investigated the impact of $AlEt_3$ and $AlEt_2Cl$ on regio and stereoselectivity, through their coordination in the proximity of the Ti atom, as shown in Figure 3. $AlEt_3$ is the compound mostly used to activate the adsorbed $TiCl_4$ species, while $AlEt_2Cl$ is the Al-alkyl species resulting from the activation event. First, we checked that both these Al-alkyls strongly coordinate on the perfect (104)-facet, which would infer strong coordination also in proximity of the step-defect. Gratifyingly, we calculated adsorption energies of 12.5 and 19.9 kcal/mol for $AlEt_3$ and $AlEt_2Cl$ on a perfect (104)-facet, which is a good result considering that DFT is known to underestimate Al-alkyl dimerization energies.[49] Indeed, it ensures Al-alkyls adsorption to the $MgCl_2$ surface, considering that the experimental $AlMe_3$ and $AlCl_3$ dimerization energy is only 10 and 15 kcal/mol per $AlMe_3$ or $AlCl_3$ unit.[50,51] Once strong coordination of the Al-alkyl species was confirmed, we investigated again stereo and regioselectivity of propene insertion. The numbers reported in Table 2 clearly indicate that the presence of the Al-alkyls increases the stereoselectivity of primary propene insertion, particularly when the growing chain is in the less hindered outward position, with $\Delta E^{\ddagger}_{Stereo}$ approaching 1 kcal/mol. Less relevant impact of the Al-alkyls is instead calculated when the growing chain is in the already somewhat stereoselective inward position. Further, with both Al-alkyls primary propene insertion remains favored, with $\Delta E^{\ddagger}_{Regio}$ always above 1 kcal/mol. In short, $TiCl_4$ adsorption on a low energy (104) step-defect, with the near unsaturated Mg atoms decorated with Al-alkyls, can yield a moderately stereoselective site, in agreement with the experiments. Test calculations via single point energy evaluations with the hybrid PBE1PBE functionals, among the best performing functionals in reproducing CCSD(T) barriers for olefin insertion and for β-H elimination in early transition metals,[52] indicates that switching from a GGA to a HGGA functional changes somehow the value of $\Delta E^{\ddagger}_{Stereo}$ and $\Delta E^{\ddagger}_{Regio}$, but the overall conclusions remain the same, see the SI.

To further validate these conclusions, reached with a relatively small cluster, we performed additional calculations using a periodic model composed by three $MgCl_2$ monolayers, with the central monolayer hosting the defect and the active site (for further information see the SI). Focusing on the naked active site, results using the periodic model are in line with those achieved with the cluster model, with a reinforcement of stereoselectivity when the growing chain is inward coordinated, due to clashes with the nearby $MgCl_2$ monolayer. As further test, we calculated the regio and stereoselectivity of the less selective active site, with the chain in the outward position, in presence of $AlEt_3$ and the BMF Lewis base. Consistently

with the results achieved with the cluster model, the presence of $AlEt_3$ molecules flanking the active site improves stereoselectivity. The presence of bulkier BMF molecules reinforcing this trend, again in agreement with the experiments.[26,28]

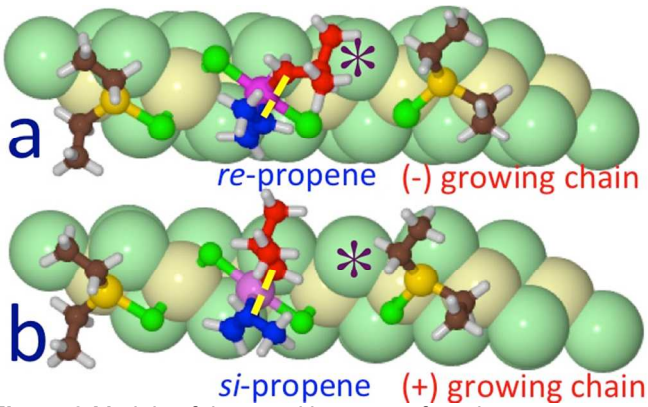

Figure 3 Models of the transition states for primary propene insertion with the growing chain in the inward coordination site. Part a, higher energy transition state, disfavored by steric interaction between the growing chain and the Cl atom marked by a star; part b, favored transition state. $MgCl_2$ in CPK, Ti-active site, propene, growing chain, $AlEt_2Cl$ in ball and stick.

In summary, $TiCl_4$ on (104)-facets presenting low energy step-defects can complement with the already known site corresponding to $TiCl_4$ on the perfect (110)-facet to explain basically all the available knowledge in ZN-catalysis. In fact, they are both potential sites for strong coordination of $TiCl_4$, and exactly the same mechanism, coordination of an Al-alkyl or a Lewis base in the proximity of the active Ti-center, can be used to confer stereoselectivity to the otherwise poorly stereoselective site. This unified mechanism is a remarkable advance in the field, since it rationalizes formation of isotactic polymer independently from the exposed facet as well as the shape and the angles between the edges of $MgCl_2$ crystallites, and suggests that further efforts should be performed to locate other low energy defects that can host a Ti-active species whose stereoselectivity can be improved by the presence of Lewis bases.

Acknowledgments.

We thank ENEA (www.enea.it) and the HPC team for support and for using ENEA-GRID and the HPC facilities CRESCO (www.cresco.enea.it) Portici (Naples), Italy.

The authors would like to dedicate this manuscript to the memory of Prof. Adolfo Zambelli, one of the fathers of stereoselective propene polymerization and co-worker of Nobel Prize Giulio Natta. He passed away in January of 2015.

Supporting Information.

Computational details, coordinates and energy of all the minimum energy discussed in the text. This material is available free of charge via the Internet at http://pubs.acs.org.

References

(1) Moore, E. P., Jr. *Polypropylene Handbook: Polymerization, Characterization, Properties, Applications*; Hanser Publishers: Munich, 1996.
(2) Natta, G. In *Nobel Lectures in Chemistry, 1963-1970*; Elsevier: 1972, p 27.
(3) Ziegler, K. In *Nobel Lectures in Chemistry, 1963-1970*; Elsevier: 1972, p 6.
(4) Resconi, L.; Cavallo, L.; Fait, A.; Piemontesi, F. *Chem. Rev.* **2000**, *100*, 1253.
(5) Seth, M.; Margl, P. M.; Ziegler, T. *Macromolecules* **2002**, *35*, 7815.
(6) Boero, M.; Parrinello, M.; Weiss, H.; Hüffer, S. *J. Phys. Chem. A* **2001**, *105*, 5096.
(7) D'Amore, M.; Credendino, R.; Budzelaar, P. H. M.; Causa, M.; Busico, V. *J. Catal.* **2012**, *286*, 103.
(8) Boero, M.; Parrinello, M.; Hüffer, S.; Weiss, H. *J. Am. Chem. Soc.* **2000**, *122*, 501.
(9) Stukalov, D. V.; Zilberberg, I. L.; Zakharov, V. A. *Macromolecules* **2009**, *42*, 8165.
(10) Correa, A.; Piemontesi, F.; Morini, G.; Cavallo, L. *Macromolecules* **2007**, *40*, 9181.
(11) Taniike, T.; Terano, M. *Macromol. Rapid Commun.* **2007**, *28*, 1918.
(12) Monaco, G.; Toto, M.; Guerra, G.; Corradini, P.; Cavallo, L. *Macromolecules* **2000**, *33*, 8953.
(13) Kuklin, M. S.; Bazhenov, A. S.; Denifl, P.; Leinonen, T.; Linnolahti, M.; Pakkanen, T. A. *Surf. Sci.* **2015**, *635*, 5.
(14) Credendino, R.; Pater, J. T. M.; Liguori, D.; Morini, G.; Cavallo, L. *J. Phys. Chem. C* **2012**, *116*, 22980.
(15) Correa, A.; Credendino, R.; Pater, J. T. M.; Morini, G.; Cavallo, L. *Macromolecules* **2012**, *45*, 3695.
(16) Credendino, R.; Pater, J. T. M.; Correa, A.; Morini, G.; Cavallo, L. *J. Phys. Chem. C* **2011**, *115*, 13322.
(17) Credendino, R.; Busico, V.; Causa, M.; Barone, V.; Budzelaar, P. H. M.; Zicovich-Wilsone, C. *PCCP* **2009**, *11*, 6525.
(18) Busico, V.; Causa, M.; Cipullo, R.; Credendino, R.; Cutillo, F.; Friederichs, N.; Lamanna, R.; Segre, A.; VanAxelCastelli, V. *J. Phys. Chem. C* **2008**, *112*, 1081.
(19) Corradini, P.; Barone, V.; Fusco, R.; Guerra, G. *Eur. Polym. J.* **1979**, *15*, 1133.
(20) Corradini, P.; Guerra, G.; Fusco, R.; Barone, V. *Eur. Polym. J.* **1980**, *16*, 835.
(21) Corradini, P.; Barone, V.; Guerra, G. *Macromolecules* **1982**, *15*, 1242.
(22) Corradini, P.; Barone, V.; Fusco, R.; Guerra, G. *Gazz. Chim. Ital.* **1983**, *113*, 601.
(23) Corradini, P.; Guerra, G.; Barone, V. *Eur. Polym. J.* **1984**, *20*, 1177.
(24) Toto, M.; Morini, G.; Guerra, G.; Corradini, P.; Cavallo, L. *Macromolecules* **2000**, *33*, 1134.
(25) Boero, M.; Parrinello, M.; Terakura, K. *J. Am. Chem. Soc.* **1998**, *120*, 2746.
(26) Chadwick, J. C.; Morini, G.; Balbontin, G.; Mingozzi, I.; Albizzati, E.; Sudmeijer, O. *Macromol. Chem. Phys.* **1997**, *198*, 1181.

(27) Sacchi, M. C.; Forlini, F.; Tritto, I.; Locatelli, P.; Morini, G.; Noristi, L.; Albizzati, E. *Macromolecules* **1996**, *29*, 3341.
(28) Morini, G.; Albizzati, E.; Balbontin, G.; Mingozzi, I.; Sacchi, M. C.; Forlini, F.; Tritto, I. *Macromolecules* **1996**, *29*, 5770.
(29) Sacchi, M. C.; Forlini, F.; Tritto, I.; Locatelli, P.; Morini, G.; Baruzzi, G.; Albizzati, E. *Macromol. Symp.* **1995**, *89*, 91.
(30) Albizzati, E.; Giannini, U.; Collina, G.; Noristi, L.; Resconi, L. In *Polypropylene Handbook*; Moore, E. P., Ed.; Hanser: Munich, 1996, p 11.
(31) Brant, P.; Speca, A. N.; Johnston, D. C. *J. Catal.* **1988**, *113*, 250.
(32) Kashiwa, N.; Yoshitake, J. *Die Makromolekulare Chemie or J. Macromol. Chem* **1984**, *185*, 1133.
(33) Paukkeri, R.; Lehtinen, A. *Polymer* **1993**, *34*, 4083.
(34) Randall, J. C. *Macromolecules* **1997**, *30*, 803.
(35) Busico, V.; Cipullo, R.; Monaco, G.; Talarico, G.; Vacatello, M.; Chadwick, J. C.; Segre, A. L.; Sudmeijer, O. *Macromolecules* **1999**, *32*, 4173.
(36) Potapov, A. G.; Kriventsov, V. V.; Kochubey, D. I.; Bukatov, G. D.; Zakharov, V. A. *Macromol. Chem. Phys.* **1997**, *198*, 3477.
(37) Jensen, V. R.; Børve, K. J.; Ystenes, M. *J. Am. Chem. Soc.* **1995**, *117*, 4109.
(38) Sakai, S. *Trends in Physical Chemistry* **1997**, *6*, 235.
(39) Puhakka, E.; Pakkanen, T. T.; Pakkanen, T. A. *J. Mol. Cat. A: Chemical* **1997**, *120*, 143.
(40) Stukalov, D. V.; Zakharov, V. A.; Popatov, A. G.; Bukatov, G. D. *J. Catal.* **2009** *266* 39.
(41) Martinsky, C.; Minot, C.; Ricart, J. M. *Surf. Sci.* **2001**, *490*, 237.
(42) Mori, H.; Sawada, M.; Higuchi, T.; Hasebe, K.; Otsuka, N.; Terano, M. *Macromol. Rapid Commun.* **1999**, *20*, 245.
(43) Andoni, A.; Chadwick, J. C.; Niemantsverdriet, H. J. W.; Thüne, P. C. *J. Catal.* **2008**, *257*, 81.
(44) Calculations using a periodic model were performed with the CP2K packege using a triple-ζ basis set and the PBE functional. Calculations of the active site with the cluster model were performed with Gaussian09 package, at the same level of theory.
(45) Bazhenov, A.; Linnolahti, M.; Pakkanen, T. A.; Denifl, P.; Leinonen, T. *J. Phys. Chem. C* **2014**, *118*, 4791.
(46) 1, N.
(47) Schlößer, D. C.; Verheij, L. K.; Rosenfeld, G.; Comsa, G. *Phys. Rev. Lett.* **1999**, *82*.
(48) Morgenstern, K.; Rosenfeld, G.; Laegsgaard, E.; Besen-Bacher, F.; Comsa, G. *Phys. Rev. Lett.* **1998**, *80*.
(49) Willis, B. G.; Jensen, K. F. *J. Phys. Chem. A* **1998**, *102*, 2613.
(50) Henrickson, C. H.; Eyman, D. P. *Inorg. Chem.* **1967**, *6*, 1461.
(51) Wade, K. *J. Chem. Educ.* **1972**, *49*, 502.
(52) Ehm, C.; Budzelaar, P. H. M.; Busico, V. *J. Organomet. Chem.* **2015**, *775*, 39.

Graphic Material for the Table of Contents